Transverse Velocity Scaling in ^{197}Au + ^{197}Au Fragmentation

J. Łukasik,[1,10] S. Hudan,[2] F. Lavaud,[3] K. Turzó,[1] G. Auger,[2] Ch.O. Bacri,[3] M.L. Begemann-Blaich,[1] N. Bellaize,[4] R. Bittiger,[1] F. Bocage,[4] B. Borderie,[3] R. Bougault,[4] B. Bouriquet,[2] Ph. Buchet,[5] J.L. Charvet,[5] A. Chbihi,[2] R. Dayras,[5] D. Doré,[5] D. Durand,[4] J.D. Frankland,[2] E. Galichet,[6] D. Gourio,[1] D. Guinet,[6] B. Hurst,[4] P. Lautesse,[6] J.L. Laville,[2] C. Leduc,[6] A. Le Fèvre,[1] R. Legrain,[5] O. Lopez,[4] U. Lynen,[1] W.F.J. Müller,[1] L. Nalpas,[5] H. Orth,[1] E. Plagnol,[3] E. Rosato,[7] A. Saija,[8] C. Sfienti,[1] C. Schwarz,[1] J.C. Steckmeyer,[4] G. Tăbăcaru,[2] B. Tamain,[4] W. Trautmann,[1] A. Trzciński,[9] E. Vient,[4] M. Vigilante,[7] C. Volant,[5] B. Zwiegliński,[9] and A.S. Botvina[1,11]

(The INDRA and ALADIN Collaborations)

[1] *Gesellschaft für Schwerionenforschung mbH, D-64291 Darmstadt, Germany*
[2] *GANIL, CEA et IN2P3-CNRS, F-14076 Caen, France*
[3] *Institut de Physique Nucléaire, IN2P3-CNRS et Université, F-91406 Orsay, France*
[4] *LPC, IN2P3-CNRS, ISMRA et Université, F-14050 Caen, France*
[5] *DAPNIA/SPhN, CEA/Saclay, F-91191 Gif sur Yvette, France*
[6] *Institut de Physique Nucléaire, IN2P3-CNRS et Université, F-69622 Villeurbanne, France*
[7] *Dipartimento di Scienze Fisiche e Sezione INFN, Univ. Federico II, I-80126 Napoli, Italy*
[8] *Dipartimento di Fisica dell' Università and INFN, I-95129 Catania, Italy*
[9] *A. Sołtan Institute for Nuclear Studies, Pl-00681 Warsaw, Poland*
[10] *H. Niewodniczański Institute of Nuclear Physics, Pl-31342 Kraków, Poland*
[11] *Institute for Nuclear Research, 117312 Moscow, Russia*

(Dated: November 11, 2003)

Invariant transverse-velocity spectra of intermediate-mass fragments were measured with the 4π multi-detector system INDRA for collisions of ^{197}Au on ^{197}Au at incident energies between 40 and 150 MeV per nucleon. Their scaling properties as a function of incident energy and atomic number Z are used to distinguish and characterize the emissions in (i) peripheral collisions at the projectile and target rapidities, and in (ii) central and (iii) peripheral collisions near mid-rapidity. The importance of dynamical effects is evident in all three cases and their origin is discussed.

PACS numbers: 25.70.Mn, 25.70.Pq, 25.40.Sc

Heavy-ion collisions in the Fermi-energy domain are rich and complex sources of fragment emissions [1]. With heavy nuclei, rather large composite systems may be formed [2–4] that represent the limit in charge and mass over which the bulk properties of excited nuclear matter may be experimentally explored with present-day means. More peripheral collisions may give access to systems consisting of low-density matter interacting with two residual nuclei. Such configurations are of interest for the study of isotopic effects in the phase behavior of the two-component nuclear fluid [5–8].

The fragment channels of both central and peripheral collisions exhibit characteristic dynamical phenomena. A collective flow, predominantly at small impact parameters, is superimposed on the thermal motion of the emitted particles and fragments, increasing in strength with the bombarding energy [9]. Peripheral collisions appear binary in the light-particle channels dominated by evaporation from the projectile and target remnants but are characterized by a strong component of fragment emission at rapidities intermediate between those of the projectile and of the target [10–16]. A possibly dynamical origin of this component, frequently termed neck emission, has been suggested but its nature has not yet been satisfactorily clarified.

A well founded understanding of the mechanisms of fragmentation processes is indispensable if their potential for investigating the thermodynamic behavior of nuclear matter is to be exploited. Considerable progress in this direction has been made possible by the advent of 4π-type detection systems that permit the construction of complete Galilei or Lorentz invariant cross-section distributions. It will be shown, in this Letter, that transverse-velocity spectra obtained from such distributions are particularly useful for identifying the qualitatively different types of emissions on the basis of their characteristic dependences on impact parameter and incident energy. A striking invariance with the incident energy is observed for mid-rapidity fragments from peripheral collisions, the fragment component whose origin is probably the least-well understood.

The data were obtained with the INDRA multidetector [17] in experiments performed at the GSI for the reaction ^{197}Au + ^{197}Au at incident energies from 40 to 150 MeV per nucleon, i.e. over a range of relative velocities from once to twice the Fermi value. Beams of ^{197}Au delivered by the heavy-ion synchrotron SIS were directed onto ^{197}Au targets of 2-mg/cm^2 areal thickness. Annular veto detectors directly upstream of the INDRA detection system and measurements with empty target frames have been employed in order to verify that the synchrotron beams were properly focussed into the 12-mm-diameter entrance hole of the 4π detection device.

The energy calibration of the 336 CsI(Tl) detectors has primarily been derived from a detector-by-detector comparison of spectra remeasured for the reaction ^{129}Xe +

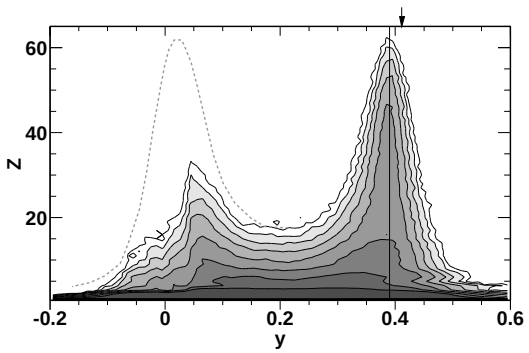

FIG. 1: Contour plot of the measured production cross sections as a function of the fragment Z and the rapidity y for the reaction ^{197}Au + ^{197}Au at 80 MeV per nucleon for semi-peripheral collisions (bin 3). The vertical line indicates the mean rapidity of heavy projectile-like fragments which is slightly below the projectile rapidity $y = 0.41$ (arrow). The dashed line is meant to visually restore the symmetry of the reaction which is disturbed by the reduced acceptance for low-energy fragments.

^{nat}Sn at 50 MeV per nucleon with spectra measured previously at GANIL [3, 13, 14]. There, calibration data had been obtained by scattering a variety of primary and secondary beams from thin targets. The light emission from the CsI(Tl) scintillators was parameterized according to Ref. [18], and the Z dependence of the parameters was obtained from comparing the generated $\Delta E - E$ maps to predictions of energy-loss and range tables [19].

As in previous investigations of symmetric heavy ion collisions [13, 14], the total transverse energy $E_\perp^{12}$ of light charged particles ($Z \leq 2$) has been used as an impact parameter selector. The $E_\perp^{12}$ spectra are found to scale linearly with the incident energy, and the scaled spectra coincide. The relation between $E_\perp^{12}$ and the reduced impact parameter $b/b_{\rm max}$, obtained with the use of the geometrical prescription [20], is linear in very good approximation, where $b/b_{\rm max}$ decreases with increasing $E_\perp^{12}$. This behavior is very similar to that observed for the ^{129}Xe + ^{nat}Sn reaction at the lower energies 25 to 50 MeV per nucleon [13, 14]. With the same prescription as used there, impact parameter bins were generated. The most central bin, labelled bin 8, covers impact parameters up to 5% of $b_{\rm max}$. The remaining part of the $E_\perp^{12}$ spectrum is divided into 7 bins of equal width, corresponding to 7 bins of approximately equal width in b. Bin 1 contains the most peripheral collisions that were registered at the trigger condition of at least three detected particles.

Peripheral collisions display a binary character in that heavy residues of the projectile and target are observed, as far as they are within the INDRA acceptance (Fig. 1). The emission of intermediate-mass fragments, however, is neither binary nor isotropic with respect to these residues (Figs. 1,2). Their intensity is heavily weighted towards mid-rapidity where, at the lower incident energies, it displays a pronounced maximum, similar as observed for

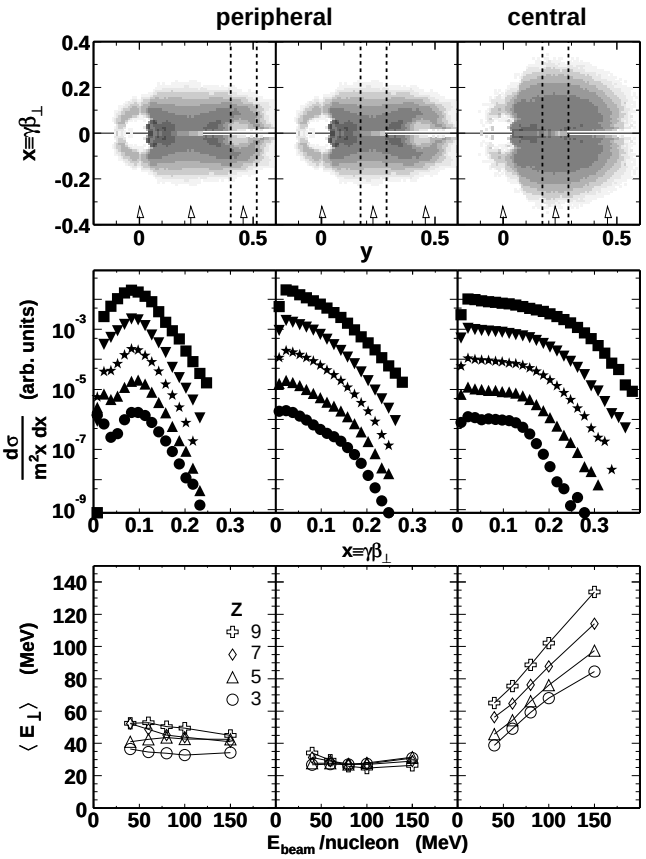

FIG. 2: Top row: invariant cross section distributions for Z = 3 fragments as a function of transverse velocity (x) and rapidity (y) for peripheral (bin 1, left and center) and central (bins 7 and 8, right) collisions of ^{197}Au + ^{197}Au at E/A = 100 MeV. The dashed lines indicate the windows in relative rapidity chosen for the data shown below; the arrows denote the rapidities of the target, the center-of-mass, and the incident projectile (from left to right).
Middle row: invariant transverse velocity spectra for $Z = 3$ at bombarding energies E/A = 40, 60, 80, 100 and 150 MeV (from bottom to top), vertically displaced for clarity and each plotted over three decades.
Bottom row: mean transverse energies $\langle E_\perp \rangle$ as a function of the incident energy for fragments with odd $Z \leq 9$ as indicated.

^{129}Xe + ^{nat}Sn [13, 14]. At higher incident energies, 100 MeV per nucleon and above, the fragment distributions start to separate at mid-rapidity, and a cross-section minimum develops (Fig. 2, top). This may be seen as the beginning of a smooth evolution into the relativistic regime where the fragment emission is concentrated at the projectile and target rapidities [21].

As a potentially useful observable for identifying the dominant mechanisms of fragment production, invariant transverse-velocity spectra for selected centrality and rapidity bins are presented in Fig. 2. These spectra are expected to be Gaussian for a thermally emitting source, with a width $\sigma^2 = T/m$ where T and m are the temperature of the source and the mass of the emitted par-

ticle, respectively. If Coulomb forces act in addition, a peak will appear near the velocity corresponding to the Coulomb energy.

The cuts in rapidity y that were used to generate the spectra are indicated in the invariant cross section plots, shown for $Z = 3$ and 100 MeV per nucleon in the upper row of Fig. 2. Identical cuts in the scaled rapidity y/y_p, with a width of 25% of y_p, were used for the other bombarding energies (y_p is the projectile rapidity). Impact-parameter bin 1 was chosen to represent peripheral collisions, and bins 7 and 8 were combined to obtain adequate statistics for central collisions. The transverse-velocity spectra of Li nuclei for the five bombarding energies are shown in the middle panels of the figure. The mean transverse energies for fragments with atomic number $Z = 3$, 5, 7, 9 as a function of the incident energy are given below.

The transverse velocities near the projectile rapidity in peripheral collisions (left column) are dominated by a prominent Coulomb peak that indicates repulsion from the surface of a heavy primary fragment. The peak velocity $\beta \approx 0.09$, equivalent to 2.7 cm/ns and typical for fragment emission from a gold-like residue [22], is rather stable and drops by only $\Delta\beta \approx 0.01$ as the energy is raised from 40 to 150 MeV per nucleon.

Coulomb peaks are absent in the emissions at midrapidity which exhibit two different scaling behaviors for the central and peripheral impact parameters. In the central case (Fig. 2, right panel), the shapes are approximately Gaussian, with an extra shoulder superimposed at the lower incident energies, most likely due to Coulomb repulsion. Both, the mean velocity and the width increase considerably with increasing bombarding energy and with the fragment mass. The mean transverse energies, correspondingly, grow approximately linearly with the incident energy but slightly slower than in proportion to the fragment mass (cf. Ref. [23]). These observations reflect the increasing collectivity of the fragment motion as the incident energy rises, a result of higher compression, a resulting stronger Coulomb acceleration, and higher temperatures of the composite sources that are initially formed in central collisions [24, 25].

The most striking behavior is observed for the midrapidity fragments from peripheral reactions (middle column of Fig. 2). The shapes of the transverse-velocity spectra, somewhat between Gaussian and exponential, are virtually the same at all incident energies, except perhaps for a weak shoulder that develops at the lowest energies (middle panel). The mean transverse energies are invariant with respect to the incident energy and to the fragment Z (bottom panel). The existence of a common energy scale for intermediate-mass fragments over the investigated wide range of bombarding energies seems, at first sight, unexpected for a dynamical mechanism and raises the question of where to search for its origin.

Kinetic energies that are independent of the particle species are expected within thermal models. In the present case, however, a mean transverse energy $\langle E_\perp \rangle \approx$ 30 MeV, corresponding to a temperature T of the same magnitude, seems rather large and clearly exceeds the temperature range at which fragments can be expected to survive. Kinetic energies that appear thermal and correspond to high temperatures are obtained from the Goldhaber model in which fragment momenta are assumed to result from the nucleonic Fermi motion [26]. This approach has proven useful for the interpretation of kinetic energies of intermediate-mass fragments from spectator decays at relativistic bombarding energies [27]. In the present case, however, the value $\langle E_\perp \rangle = T = 15$ MeV, derived for the Fermi momentum $p_F = 265$ MeV/c of heavy nuclei, amounts to only about half of the equivalent temperature that is required (Fig. 3). Since it is unlikely that the density or the temperature of the neck region attain the extreme values that would be needed to bring this value up and close to observation [28], at most part of the observed energies can be ascribed to the intrinsic nucleonic motion.

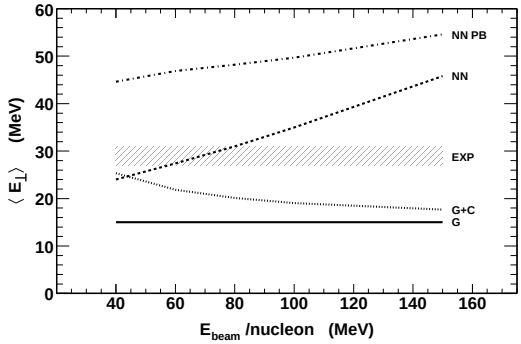

FIG. 3: Mean transverse energies $\langle E_\perp \rangle$ as obtained from the Goldhaber model for $p_F = 265$ MeV/c (full line labelled G), after adding the Coulomb energy (dotted line, G+C), and for nucleons from primary nucleon-nucleon collisions with (dashed-dotted line, NN PB) and without (dashed line, NN) considering Pauli blocking. The experimental result for midrapidity fragments from peripheral collisions is represented by the hatched area.

The intermediate bombarding energies are characterized by the interplay of mean-field and nucleon-nucleon collision dynamics. The importance of the latter increases with energy, due to the reduced role of Pauli blocking, as apparent in the prompt emissions of light particles [15, 29]. The transverse energies generated in primary nucleon-nucleon collisions should reflect the incident energy, in addition to the Fermi motion. The rise with energy, however, will be partly compensated by the reduced Pauli blocking of final states with low transverse momentum at higher incident energies. Simulations confirm that essentially only the widths of the distributions increase while the mean transverse energies rise rather slowly if the blocking effect is taken into account (Fig. 3). This property of the mean transverse energies is specific for the present range of energies at and above the Fermi value. Fragments formed by a coalescence mech-

anism from only scattered nucleons will have transverse energies that are clearly too high. It will be sufficient if a few of them are built into the nascent fragments which may also trigger their separation from the bulk.

The stronger Pauli blocking at the lower incident energies thus represents a compensating mechanism that contributes to the observed invariance of $\langle E_\perp \rangle$. This is also the case for the Coulomb potential generated by the two residues in the neck region. Essential for reactions at lower energies and in fission [7, 16, 30], its role is expected to decrease at the higher bombarding energies at which the residue velocities are comparable to or larger than those of the mid-rapidity fragments. Simulations with Coulomb trajectory calculations confirm this effect (Fig. 3). They also indicate that the Coulomb contribution to the transverse energy may depend very little on the fragment Z. In the simulations, a thermal distribution was assumed for the initial fragment motion, in accordance with the Goldhaber model. It has the consequence that heavier fragments move away more slowly from the field free zone in between the receding residues. This may explain why the Coulomb forces do not disturb the Z invariance of the transverse motion (Fig. 2 bottom, middle panel).

All these mechanisms, whose effects are schematically illustrated in Fig. 3, are contained in realistic microscopic transport theories which thus seem suited to test the suggested reason for the observed invariances [31]. Complications may arise from the fact that surface effects and finer details in the modelling are important in peripheral reactions and will require a rather careful treatment [14, 32]. Additional insight, in particular with regard to the role of the Coulomb forces, may also be gained from an experimental study of the dependence of the fragment transverse motion on the mass of the collision system.

To summarize, three different modes of fragment emission have been characterized on the basis of the transverse-velocity spectra. All of them are strongly influenced by dynamical effects. Peripheral collisions appear binary only as long as the heavy residues and evaporated light particles are considered. The emission of intermediate-mass fragments is not symmetric with respect to the residue rapidities. The mid-rapidity fragments from these collisions exhibit large transverse velocities on a scale corresponding to an effective temperature of nearly 30 MeV. The invariance of their transverse motion with incident energy and fragment Z is most likely the result of a compensation of several dynamical effects, the initial Fermi motion in the colliding nuclei, the generation of transverse momenta in nucleon-nucleon collisions and the Coulomb interaction between the fragments and the separating residues. The important role of collective motion, linearly increasing with the incident energy over the covered range, is evident for central collisions.

The authors would like to thank the staff of the GSI for providing heavy ion beams of the highest quality and for technical support. M.B. and C.Sc. acknowledge the financial support of the Deutsche Forschungsgemeinschaft under the Contract No. Be1634/1- and Schw510/2-1, respectively; D.Go. and C.Sf. acknowledge the receipt of Alexander-von-Humboldt fellowships. This work was supported by the European Community under contract ERBFMGECT950083.

[1] For recent reviews of the field see, e.g., *Proceedings of the International Workshop XXVII on Gross Properties of Nuclei and Nuclear Excitations, Hirschegg, Austria*, edited by H. Feldmeier *et al.* (GSI, Darmstadt, 1999); D. Durand, E. Suraud, and B. Tamain, *Nuclear Dynamics in the Nucleonic Regime*, ISBN 0750305371 (Institute of Physics, Bristol and Philadelphia, 2001).
[2] M. D'Agostino *et al.*, Phys. Lett. B **368**, 259 (1996).
[3] N. Marie *et al.*, Phys. Lett. B **391**, 15 (1997).
[4] J.D. Frankland *et al.*, Nucl. Phys. **A689**, 940 (2001).
[5] H. Müller and B.D. Serot, Phys. Rev. C **52**, 2072 (1995).
[6] L. Shi and P. Danielewicz, Europhys. Lett. **51**, 34 (2000).
[7] G. Poggi, Nucl. Phys. **A685**, 296c (2001).
[8] V. Baran *et al.*, Nucl. Phys. **A703**, 603 (2002).
[9] W. Reisdorf and H.G. Ritter, Ann. Rev. Nucl. Part. Science **47**, 663 (1997).
[10] C.P. Montoya *et al.*, Phys. Rev. Lett. **73**, 3070 (1994).
[11] J. Tõke *et al.*, Phys. Rev. Lett. **75**, 2920 (1995).
[12] J.F. Dempsey *et al.*, Phys. Rev. C **54**, 1710 (1996).
[13] J. Łukasik *et al.*, Phys. Rev. C **55**, 1906 (1997).
[14] E. Plagnol *et al.*, Phys. Rev. C **61**, 014606 (2000).
[15] D. Doré *et al.*, Phys. Rev. C **63**, 034612 (2001).
[16] S. Piantelli *et al.*, Phys. Rev. Lett. **88**, 052701 (2002).
[17] J. Pouthas *et al.*, Nucl. Instr. Meth. in Phys. Res. **A357**, 418 (1995).
[18] Pârlog *et al.*, Nucl. Instr. Meth. in Phys. Res. **A482**, 693 (2002).
[19] F. Hubert, R. Bimbot, and H. Gauvin, Atomic Data Nucl. Data Tables **46**, 1 (1990).
[20] C. Cavata *et al.*, Phys. Rev. C **42**, 1760 (1990).
[21] A. Schüttauf *et al.*, Nucl. Phys. **A607**, 457 (1996).
[22] R. Trockel *et al.*, Phys. Rev. Lett. **59**, 2844 (1987).
[23] W.C. Hsi *et al.*, Phys. Rev. Lett. **73**, 3367 (1994).
[24] R. Nebauer and J. Aichelin, Nucl. Phys. **A650**, 65 (1999).
[25] F. Lavaud *et al.*, in *Proceedings of the INPC 2001, Berkeley, California* edited by E. Norman *et al.* (American Institute of Physics, New York, 2002), p. 716.
[26] A.S. Goldhaber, Phys. Lett. **53B**, 306 (1974).
[27] T. Odeh *et al.*, Phys. Rev. Lett. **84**, 4557 (2000).
[28] W. Bauer, Phys. Rev. C **51**, 803 (1995).
[29] R.C. Lemmon *et al.*, Phys. Lett. B **446**, 197 (1999).
[30] D.E. Fields *et al.*, Phys. Rev. Lett. **69**, 3713 (1992).
[31] see, e.g., the AMD analysis of inclusive transverse-energy spectra in ^{64}Zn + ^{58}Ni by R. Wada *et al.*, Phys. Rev. C **62**, 034601 (2000).
[32] J. Aichelin, Phys. Rep. **202**, 233 (1991).